

Research Article

WiFi-Based Indoor Positioning and Communication: Empirical Model and Theoretical Analysis

Zhaoyang Han,¹ Ziyue Wang,¹ Huakun Huang ,² Lingjun Zhao,³ and Chunhua Su ¹

¹School of Computer Science and Technology, University of Aizu, Fukushima, Japan

²School of Computer Science and Cyber Engineering, Guangzhou University, Guangzhou, China

³School of Software Engineering, Sun Yet-Sen University, Guangzhou, China

Correspondence should be addressed to Huakun Huang; huanghuakun@gzhu.edu.cn and Chunhua Su; chsu@u-aizu.ac.jp

Received 30 March 2022; Revised 4 May 2022; Accepted 6 May 2022; Published 6 June 2022

Academic Editor: Kuruva Lakshmana

Copyright © 2022 Zhaoyang Han et al. This is an open access article distributed under the Creative Commons Attribution License, which permits unrestricted use, distribution, and reproduction in any medium, provided the original work is properly cited.

GPS (Global Positioning System) has been developed more mature and perfect in outdoor positioning. However, because GPS signals cannot be effectively transmitted in a complex indoor environment, positioning and navigation cannot be performed in typical situations such as indoor emergency occurrence location determination, shopping mall guides, and intelligent service robot fixed-point services. With the deepening of related researches, technologies based on ultrasound, WiFi, Bluetooth, radio frequency identification, infrared, etc. have been used to achieve indoor target positioning. The traditional WiFi-based indoor positioning technology uses the RSS value and CSI value of the WiFi signal to build a fingerprint database for positioning. The algorithm is complex and highly cost, and the function is relatively single. In this paper, for the first time, we propose a new algorithm for integrating indoor target positioning and communication based on WiFi signals. Using RSS value of WiFi signal for target location and using CSI value for indoor wireless channel modeling to get the system transmission function to achieve communication purpose, the experimental results show that the positioning algorithm can achieve positioning within the ideal accuracy range, and the communication algorithm part can accurately recover the system function of the wireless multipath channel and finally achieve the goal of integration of positioning and communication based on the WiFi signal level.

1. Introduction

1.1. Background. With the rapid development of the wireless communication, mobile internet technology has been steadily matured and gradually completed in recent years [1, 2]. Since positioning service is able to provide more accurate time information and space information, improve user experience, ensure the property safety of people in all walks of life, and promote the development of the information society, it can be regarded as one of the most successful applications of the mobile internet technology, which has been paid more and more attention. On the one hand, outdoor positioning technology has made great progress, where Global Positioning System (GPS) technology has been widely used due to its performance of low latency, ideal accuracy, and high resolution [3–5]. However, since GPS positioning technology severely relies on signals propagating

in the air, the complex environment indoors hinder the signal's propagation, and GPS's applicability is severely limited in the indoor environment. On the other hand, as for the indoor positioning aspect, there are many types of technologies to realize the indoor positioning, such as ultrasonic [6], infrared [7], sensor [8], RFID [9], WiFi [10], UWB [10], and Bluetooth [11, 12], whose comparison of advantages and limitation are presented in Table 1. Note that despite different positioning method is with different complexity and cost of implementation, low cost and widely use characteristics make WiFi-based approach a more promising indoor positioning technology. Furthermore, though most algorithms and technologies can achieve the goal of indoor positioning, how to maximize the indoor wireless signal's utilization, e.g., joint positioning and communication with indoor wireless signal [13], while keeping certain positioning accuracy has not been fully considered and investigated.

TABLE 1: Comparison of different positioning technology.

| Name | Advantages | Limitations |
|------------------------|---|--|
| Ultrasonic positioning | The equipment is simple, and the measurement results have high accuracy. | Affected by NLOS, the hardware requirements are high, and the cost is high. |
| Infrared positioning | Does not spread during transmission. | Affected by NLOS, the transmission distance is limited. |
| RFID positioning | The system structure and measurement principle are simple. | Accuracy is directly proportional to system complexity. |
| UWB positioning | Low power consumption, strong anti-interference, and low system complexity. | Requires strict clock synchronization at the sender and receiver, and the hardware cost is high. |
| WiFi positioning | Simple equipment, low cost, and common implementation difficulty | Low accuracy and lack of effective use of signals. |

1.2. Related Works. As one indispensable metric of the WiFi signal, received signal strength (RSS) could reflect the geometry distribution of the transmitted signal, where the larger RSS value is, the closer the target is to the transmitter. Based on such theory, the WiFi-based indoor positioning approach is put forward, which relates the target's position with the RSS value by establishing the WiFi-based signal fingerprinting databased. At this time, the position of the target can be estimated by comparing the current RSS value with the established fingerprinting. Up to now, lots of efforts have been made on the RSS-based WiFi indoor positioning technology, for example, Huang et al. [14] analyzed the reasons for moving objects' positioning errors in the RSS-based positioning approach, where a motion speed and Kalman filtering-based weighted filtering algorithm is proposed. The new fusion algorithm performs better than traditional Kalman filtering algorithms, whose positioning error can be greatly reduced [15]. Ma et al. [16] put forward the online and offline positioning method based on the traditional fingerprint positioning algorithm, whose experimental results show that the weighted fusion of the two positioning results can be more accurate than the WKNN and joint probability algorithm. Given the limitations of the traditional WKNN algorithm, Wang et al. [17] proposed an improved algorithm based on the RSS fingerprint database, where the positioning accuracy can be enhanced by the proposed algorithm to some extent. In [18], Deng et al. proposed an improved fusion algorithm based on Kalman filtering, and the positioning accuracy of the proposed algorithm is higher than that of the WiFi-based positioning algorithm. In [19], Hsieh et al. used the deep learning method to derive the RSS and CSI values of WiFi signals, by which the positioning accuracy can be enhanced compared to the traditional positioning algorithms. Yu et al. [20] solved the problem of inaccurate RSS data sources, where a practical algorithm for extracting RSS information is proposed. Besides, experimental results show that the positioning accuracy of the algorithm can reach 1.5m. Lembo et al. [21] gave the detailed analysis on the RSS measurement at the physical structure level and combined the neural network algorithm to improve positioning accuracy, which is proved to meet the needs of ideal positioning errors compared with the typical baselines. In the scenario where a smartphone is used indoors, Guo et al. put up an RTT-RSS-based ranking algorithm with WiFi signals, and the experiment results show

that the algorithm's accuracy can reach 1.435 m. Shu et al. [22] proposed a prediction algorithm based on indoor WiFi data's queuing time, whose experimental results show that the proposed wheel model is consistent with the theoretical analysis and has strong applicability. Yang and Shao [10] proposed a high-resolution time of arrival (ToA) estimation algorithm, and compared with the traditional algorithms, the experimental results of the positioning performance are improved.

In terms of communication function of the WiFi signal, it can be realized based on the CIS information. Specifically, with the help of CIS value, after modeling the indoor wireless channel, the transmission function of the wireless communication system can be derived to complete the communication function. So far, many researchers have devoted themselves to the CSI-based communication realization; for example, in [23], after analyzing the classical wireless channel modeling method, Michelson et al. put forward the multiple factor-based wireless channel modeling algorithm due to the needs in real life. And the experiment results show that the proposal can trade off theory and practice of communication function well. Kumar et al. [24] proposed a wireless channel model in the indoor single-input and single-output (SISO) scenario, where the experiment results show that the proposed model can play an essential role in broadband mobile communications. Xu et al. [25] modeled the wireless channel under the conditions of multiple transmissions and multiple receptions, and experiments prove that the model can reflect the state of the wireless channel to a certain extent. Kalachikov and Shelkunov [26] used a matrix analysis method to analyze the wireless channel model in the multi-input and multioutput (MIMO) scene in theory. The results show that the designed model is more in line with the characteristics of actual measured values than the traditional model. Stridh et al. [27] modeled the MIMO channel at 5.8 GHz, where the experimental results show that the established model is feasible. Liu et al. [28] gave the model of the wireless channel from the perspective of a Markov chain, and the experimental results show that although the model can meet the practical requirements under various parameter settings.

In summary, despite RSS-based approaches can realize the indoor positioning with WiFi signal, the tradeoff between high positioning accuracy, smaller positioning error, and less implement cost is difficult to achieve.

Moreover, the wireless channel function can be estimated with the CSI information, but the proposed model has not been comprehensively analyzed and proofed in theory. Therefore, from the viewpoints of numerical results and theoretical analysis, the joint indoor positioning and communication based on RSS and CSI of WiFi signal have not been taken into consideration, which would be the work of this paper.

1.3. Motivation and Contribution. Based on the above analysis, to address this problem, this paper is aimed at proposing one WiFi-based indoor positioning and communication scheme, where RSS information is used to achieve the positioning goal and communication function is realized with the help of CSI information. The main contribution of this paper can be summarized as follows:

- (1) To achieve the indoor positioning goal with WiFi technology, the RSS information is utilized, where an empirical model is established to replace the traditional fingerprinting database with the curve fitting approach
- (2) To realize the WiFi-based indoor communication target, we establish the wireless channel modeling under the SISO and OFDM-based MIMO scenarios, respectively, where the proposal is proved to be feasible given the environment noise existence
- (3) To evaluate the feasibility and performance of the proposal, numerical experiments are conducted, and the results have shown that when compared with other benchmarks, the proposed method can achieve smaller positioning error with less implementation cost

1.4. Outline of the Paper. The rest of this paper is organized as follows. In Section 2, the typical indoor positioning technologies are introduced from three aspects, i.e., ToA-based positioning, TDoA-based positioning, and CSI-based positioning. Section 3 establishes the system model and formulates the problem, where RSS-based positioning model and Kalman filtering model are detailed. Section 4 gives the empirical model-based indoor positioning scheme with WiFi, where the collection and process steps of RSS data are presented. In Section 5, the theoretical analysis for WiFi-based indoor communication is given, where the derivations of wireless channels are detailed from SISO and OFDM-based MIMO scenarios, respectively. The numerical experiments are conducted in Section 6, where indoor positioning performance is evaluated with numerical results and indoor communication function is verified in theory. Finally, a brief conclusion is given to summarize the whole paper in Section 7.

2. Typical Indoor Positioning Technology

2.1. ToA-Based Indoor Positioning. The round-trip time (RTT) refers to the time between the transmitter and the receiver. With the help of RTT, the distance between the

transmitter and the receiver can be obtained by multiplying half of RTT and the signal propagation speed. Figure 1 shows the principle of time of arrival- (ToA-) based positioning. As shown in Figure 1, MP indicates the object's position to be determined; AP_1 , AP_2 , and AP_3 indicate three access points, respectively. According to the measured RTT value, the values of d_1 , d_2 , and d_3 can be calculated. Denote the positioning information of AP_1 , AP_2 , AP_3 , and MP as $AP_1(x_1, y_1)$, $AP_2(x_2, y_2)$, $AP_3(x_3, y_3)$, $MP(x, y)$, respectively. Hence, the position of MP can be solved by combining the following equation:

$$\begin{aligned} (x - x_1)^2 + (y - y_1)^2 &= d_1^2, \\ (x - x_2)^2 + (y - y_2)^2 &= d_2^2, \\ (x - x_3)^2 + (y - y_3)^2 &= d_3^2. \end{aligned} \quad (1)$$

Moreover, it should be noted that despite the ToA-based positioning approach is with simple operation and needs no complex transmitting and receiving equipment, it still faces some challenges, such as low positioning accuracy, high positioning error, and strict requirement time synchronization for the transmitter and receiver.

2.2. TDoA-Based Indoor Positioning. In the Time Difference of Arrival (TDOA) scheme, the node to be located directly sends two different signals to the reference node that has been set in advance. Compared with ToA-based positioning scheme, there is no need to perform strict time synchronization on the transmitting and receiving end, and only the arrival time to the reference node for the two different signals needs to be measured. At this time, the distance between the transmitter and the receiver can be obtained by multiplying the half difference time and the signal's propagation speed. Figure 2 depicts the principle of TDoA-based positioning technology. As shown in Figure 2, MP indicates the object's position to be estimated. AP_1 , AP_2 , and AP_3 indicate three access points with known position information. Hence, the three access points can make up a hyperbolic line with two random access points as focus. Since MP must be inside a triangle formed by AP_1 , AP_2 , and AP_3 , the position of MP can be derived by solving the intersection of the three hyperbolic lines.

In addition, the advantage of TDoA-based positioning is that there is no need for strict time synchronization, and the hardware equipment at the receiving end is simple. However, its limitation is that the transmitter needs to be able to send two different signals.

2.3. CSI-Based Indoor Positioning. Due to the time variability of the wireless channel, the multipath effect will also change with time going by. To depict the characteristic of the wireless channel model, indicators including the time delay, frequency attenuation, and Doppler frequency shift generated on all paths are adopted to establish the wireless channel model, which is further represented by the channel impulse response (CIR) function. When the spectrum of the received and transmitted signals is known, the channel frequency response (CFR) which reflects the multipath characteristics

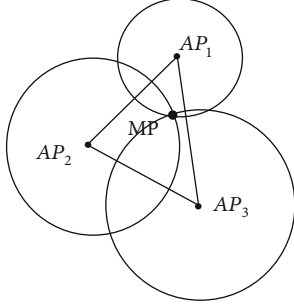


FIGURE 1: Principle of ToA-based positioning.

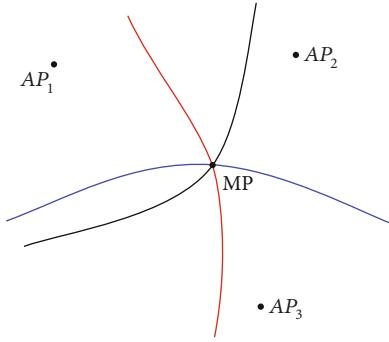


FIGURE 2: Principle of TDoA-based positioning.

of the channel can be calculated. Then, based on the inverse Fourier transform (IFT) approach, the CIR can be calculated, where channel state information (CSI) is the sample version of CIR/CFR under one specific transmission protocol.

To be specific, in the CSI-based indoor positioning scene, according to the signal attenuation during propagation, the channel model for signal propagation can be established. After combining the environmental factors in different scenarios, the position information of the target point can be estimated through related operations. In summary, the advantage of CSI-based indoor positioning is that the multipath propagation of signals can be better solved and characterized. However, the complex mathematical model and workload of signal processing also hinder the implement of this scheme.

3. System Model and Problem Formulation

3.1. RSS-Based Positioning Model. In the RSS-based positioning scheme, the premise is to establish the fingerprinting database of the WiFi signal, where the RSS value can be related to the geometry position. Then, for the target object to be located, we only need to measure the RSS value and compare such value with the fingerprinting database to estimate the position by the matching algorithm. Specifically, in the indoor environment, the sum of multipath signals can be expressed as follows:

$$V = \sum_{i=1}^N |V_i| e^{-j\theta_i t}, \quad (2)$$

where $|V_i|$ and $|\theta_i|$ represent the amplitude and phase of the i th path's signal and N is the total number of paths. At this time, the RSS value can be calculated as follows:

$$\text{RSSI} = 20 \log_{10} |V|. \quad (3)$$

Without loss of generality, on the one hand, when the target object is within the plane of two dimensions, at least three access points, i.e., anchor points, with known position need to be placed in advance. On the other hand, if the target locates at the space of three dimensions, there are at least four access points with known position deployed in the indoor environment [29].

3.2. Kalman Filtering Algorithm. In the wireless communication system, the Kalman filtering algorithm can reduce the errors resulted from the environment noise. As far as the Kalman filtering algorithm is concerned, based on the measured value in the current data and the predicted value and error at the previous moment, it can calculate the current optimal amount and predict the data value at the next moment. It should be noted that the error is included in the calculation process, which is specifically divided into prediction error and measurement error, i.e., noise. Besides, the errors exist independently and are not always affected by data measurement. To be specific, the general form of the Kalman filtering algorithm is detailed as the following five steps. where \hat{x}_{k-1} and \hat{x}_k represent the posterior state estimates at time $k-1$ and k , respectively; \hat{x}_k^- represents the prior state estimates at time k ; P_k denotes the posterior estimate covariance at k ; and P_k^- represents the prior estimate covariance at k .

Step 1. One step prediction equation of state:

$$\hat{x}_k^- = A\hat{x}_{k-1} + Bu_{k-1}. \quad (4)$$

Step 2. One-step prediction of mean square error:

$$P_k^- = AP_{k-1}A^T + Q. \quad (5)$$

Step 3. Filter gain equation (weight):

$$H_k = \frac{P_k^- H^T}{HP_k^- H^T + R}. \quad (6)$$

Step 4. Filter estimation equation (optimal value):

$$\hat{x}_k = \hat{x}_k^- + K_k(Z_k - H\hat{x}_k^-). \quad (7)$$

Step 5. Filter the mean square error update matrix:

$$P_k = (I - K_k H)P_k^-, \quad (8)$$

Meanwhile, H is the transformation matrix from state variables to observations, Z_k represents the measured value, K_k represents the filter gain matrix, A represents the state transition matrix, Q represents the covariance of the system excitation process, R represents the measurement noise

covariance, and B represents the matrix that converts the input to the state.

3.3. Problem Formulation. Based on the above established models and analysis, in the indoor environment, the goal of this paper is to minimize the positioning error with less implementation cost, which is based on the RSS value of the WiFi signal, and maintain the communication function according to the WiFi signal's CSI information at the same time.

4. Empirical Model-Based Indoor Positioning with WiFi

4.1. Basic Idea. In this section, to realize the indoor positioning with WiFi signal's RSS value, one empirical model-based positioning scheme is put forward. Specifically, we firstly determine the indoor environment for RSS data collection. Then, after Gaussian filtering and Kalman filtering, linear coding of the original data is adopted to improve the reliability of the data. Finally, we use the processed RSS data to construct the empirical model, where the least square method is used to obtain the optimal positioning model.

4.2. Data Collection. To meet the needs of minimum positioning accuracy, the indoor environment should be divided accordingly, where the size of the grid points can directly influence the positioning accuracy. As is known that two-dimensional plane positioning technology requires three access nodes, and three border nodes are selected as access nodes in the grid. At each grid point, we measure and record the grid's RSS values, which are from three access nodes in turn. Each grid point is measured 100 times to eliminate the influence of measurement errors on the data.

4.3. Data Processing. There are two main steps in the data processing stage. To be specific, at first, the collected RSS data is processed with the Gaussian and Kalman double filtering operations. Then, we perform linear coding operation on the filtered data, by which the influence brought by the equipment difference can be eliminated.

4.4. Curve Fitting-Based Empirical Model. In this subsection, the curve fitting-based empirical model is adopted to realize the RSS-based indoor positioning. In general, three major operations are performed by the following steps:

Step 1. Construct appropriate empirical models (i.e., Gaussian fit, polynomial fit, and double exponential fit).

Step 2. Adopt the least squares to perform the fit test.

Step 3. Add weight to the established empirical model, which can improve the reliability of the data.

Mathematically, the above illustrations can be further expressed as the following four steps:

Step 1. Deploy M access nodes in the indoor environment, and divide the measurement site into N grid points. Hence, there are M sets of raw RSS data, i.e.,

$$A = \begin{pmatrix} A_1 \\ \vdots \\ A_M \end{pmatrix} = \begin{pmatrix} (x_1, y_1, \text{RSS}_{A_1}(1)) & \cdots & (x_N, y_N, \text{RSS}_{A_1}(N)) \\ \vdots & \ddots & \vdots \\ (x_1, y_1, \text{RSS}_{A_M}(1)) & \cdots & (x_N, y_N, \text{RSS}_{A_M}(N)) \end{pmatrix}. \quad (9)$$

Step 2. After performing the double filtering, linear coding, and other signal processing operations, the RSS data can be denoted as follows:

$$A' = F \cdots C \cdots A, \quad (10)$$

where F is the filtering process and C represents the linear encoding process.

Step 3. Establish the relationship between the processed RSS data and the geometry position of the measured grid points, which is expressed as follows:

$$Y = \begin{pmatrix} \text{RSS}_{A_1} \\ \vdots \\ \text{RSS}_{A_M} \end{pmatrix} = g \begin{pmatrix} (x_1, y_1) & \cdots & (x_N, y_N) \\ \vdots & \ddots & \vdots \\ (x_1, y_1) & \cdots & (x_N, y_N) \end{pmatrix}. \quad (11)$$

Among them, g represents the mapping relationship of functions.

Step 4. Determine the weighting coefficient of each RSS function, mathematically,

$$(x_i, y_i) = K \cdot g^{-1}[Y], \quad (12)$$

where K is a matrix of weighting coefficients, and

$$K = \begin{pmatrix} k_1 \\ \vdots \\ k_m \end{pmatrix}, \quad (13)$$

$$k_i = \frac{\text{RSS}_i(i)}{\sum_{j=1}^n \text{RSS}_j(j)}.$$

5. Theoretical Analysis for WiFi-Based Indoor Communication

In this section, we use theoretical analysis to derive the mathematical expression of the indoor wireless channel transmission function. Besides, we also optimize the derived transmission function by considering the noise and inter-channel effects in theory. At last, a more applicable transmission function model is derived in the mathematical form.

5.1. Wireless Channel Modeling in SISO Scenario. As shown in Figure 3, the wireless channel model of SISO scenario is presented. When there are n paths in the wireless channel, the expression of the CIR function $h(t)$ can be further

written as follows:

$$h(t) = [\alpha_1, \alpha_2, \alpha_3 \cdots \alpha_n] \cdot \begin{pmatrix} \delta(t - \tau_1) & & 0 \\ & \ddots & \\ 0 & & \delta(t - \tau_n) \end{pmatrix} \cdot [e^{-j2\pi f_{q_1} t}, e^{-j2\pi f_{q_2} t}, e^{-j2\pi f_{q_3} t}, \dots, e^{-j2\pi f_{q_n} t}] = \alpha \cdot \delta \cdot f_d, \quad (14)$$

where the matrix α represents the fading, the matrix δ means the delay, and the matrix f_d represents the Doppler frequency shift generated on the propagation path.

5.2. Wireless Channel Modeling in OFDM-Based MIMO Scenario. Multiple orthogonal subcarrier signals are used in the orthogonal frequency division multiplexing (OFDM) technology, where the data is divided into several subdata streams, thereby reducing the transmission rate of the subdata streams. Then, the divided data is utilized to modulate several carriers, respectively, which is essentially a frequency division multiplexing technology. In summary, OFDM can effectively resist the effects of multipath.

Assume that the input signal is $x(t)$, after analog-to-digital conversion, $x(n)$ is obtained. Specifically, when the number of subcarriers is N , after serial-to-parallel transformation, a set of sequences with the same number of subcarriers (N) is obtained, i.e., $x_1(n), x_2(n), x_3(n) \cdots x_N(n)$. After the carrier modulation operation (which is performed by IFFT in OFDM), the data is sent to the wireless channel. Since there are many multipaths of the wireless channel, M is selected as the main object of the channel modeling (the energy proportion of these M paths should reach more than 80% of the total energy). At this time, the attenuate and delay of OFDM symbols are performed by the M paths the accordingly. Finally, the signal is sampled at the receiving end to obtain various sets of CSI values, where CSI values contains the corresponding phase and amplitude information of each subcarrier. Mathematically,

$$x(t) \xrightarrow{A/D} \begin{cases} x_1(n) \\ x_2(n) \\ x_3(n) \\ \vdots \\ x_N(n) \end{cases} \xrightarrow{\text{wireless channel}} \begin{cases} \text{CSI}_1 : \alpha_1 e^{j2\pi(f_1 + \tau_1)}, \alpha_2 e^{j2\pi(f_2 + \tau_2)}, \dots, \alpha_M e^{j2\pi(f_1 + \tau_M)}, \\ \text{CSI}_2 : \alpha_1 e^{j2\pi(f_2 + \tau_1)}, \alpha_2 e^{j2\pi(f_2 + \tau_2)}, \dots, \alpha_M e^{j2\pi(f_2 + \tau_M)}, \\ \text{CSI}_3 : \alpha_1 e^{j2\pi(f_3 + \tau_1)}, \alpha_2 e^{j2\pi(f_3 + \tau_2)}, \dots, \alpha_M e^{j2\pi(f_3 + \tau_M)}, \\ \vdots \\ \text{CSI}_M : \alpha_1 e^{j2\pi(f_M + \tau_1)}, \alpha_2 e^{j2\pi(f_M + \tau_2)}, \dots, \alpha_M e^{j2\pi(f_M + \tau_M)}. \end{cases} \quad (15)$$

In addition, the above process can be further expressed as follows:

$$[X \cdot S] * [\alpha \cdot H] = Y, \quad (16)$$

where the $*$ sign indicates a convolution operation, X represents an original signal, S means a serial-to-parallel transformation, α is fading on each path, and system transfer function is denoted by H .

As shown in Figure 4, in a MIMO system, when the i th antenna in the transmitting end is selected to send the data and the j th antenna is in charge of receiving signals in the receiving end, at this time, the state of sending and receiving can be viewed as the process of using OFDM technology under the SISO condition. When p transmitting antennas and q receiving antennas are adopted, the expression of the sending signal is

$$X(t) = [x_1^T(t), x_2^T(t), x_3^T(t) \cdots x_p^T(t)]^T. \quad (17)$$

The expression of the received signal is

$$Y(t) = [y_1^T(t), y_2^T(t), y_3^T(t) \cdots y_q^T(t)]^T. \quad (18)$$

Hence, the CSI at this time can be expressed as follows:

$$Y(t) = [y_1^T(t), y_2^T(t), y_3^T(t) \cdots y_q^T(t)]^T, \quad (19)$$

where h_{pq} is a complex number representing the amplitude and phase of the subcarriers in the antenna stream. Besides, the above process can also be expressed in the matrix form as follows:

$$H(f_k) = \begin{pmatrix} h_{11} & h_{12} & \cdots & h_{1q} \\ h_{21} & h_{22} & \cdots & h_{2q} \\ \cdots & \cdots & \cdots & \cdots \\ h_{p1} & h_{p2} & & h_{pq} \end{pmatrix}. \quad (20)$$

In summary, the i th antenna transmits data and the j th antenna receives information. After the above analysis, the system transfer functions of LOS and several other non-LOS paths can be obtained. Under the premise of transmitting signals at a known transmitting end, by performing convolving the transmitting signal with the transmission function, the received signal can be obtained.

6. Evaluation Results and Performance Analysis

6.1. Experiment Settings. The RSS-based indoor positioning experiment is conducted in the aisle. Besides, the experimental mobile device is the smartphone with android [30, 31]. Figure 5 shows the measurement of different signal's RSS values, where the interface is the screenshot of smartphone application named WiFi ANALYSIS ASSISTANT, and the deployment of the access points is shown in Figure 6.

6.2. Indoor Positioning Performance Evaluation with Numerical Results. After Gaussian filtering and Kalman filtering processing, the position of each point in the aisle is represented by two-dimensional coordinates, and the best RSS value corresponding to each point is obtained. The RSS value of different position is presented in Table 2.

At this time, after adopting the curve fitting-based approach, we can draw the three-dimensional images of

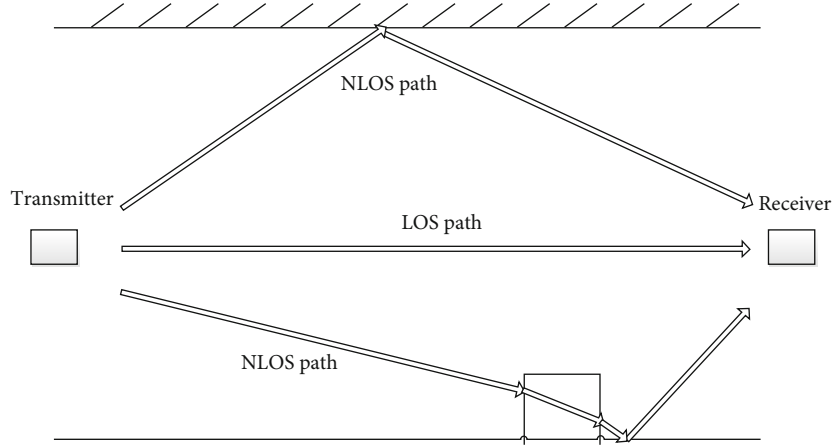


FIGURE 3: Wireless channel model of SISO scenario.

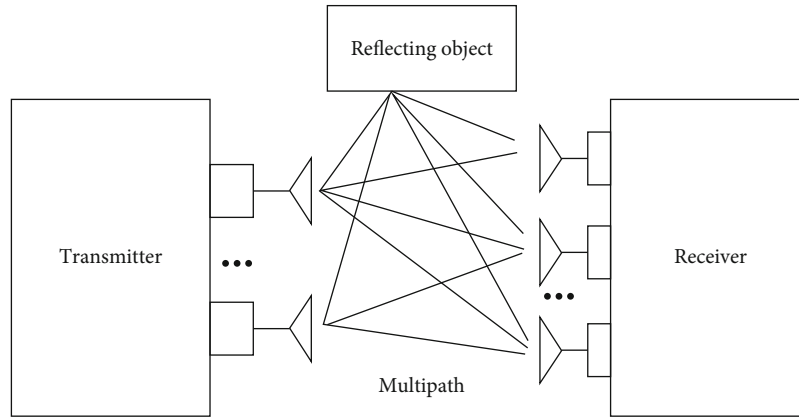


FIGURE 4: Wireless channel model of MIMO.

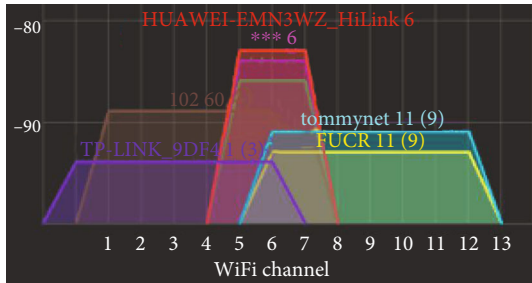


FIGURE 5: The interface of different signal RSS value.

the coordinates and the RSS values of each measured point separately. For ease of presentation, we have taken the absolute value of the signal strength.

It can be seen from Figures 7–9, that after the fitting process, the three graphs, respectively, represent the functions between the RSS of access point O , RSS of access point A , RSS of access point B , and the geometry coordinates (x, y) of the plane. To be specific, the upper half of the figure shows the three-dimensional relationship, and the lower half shows the top view. From these results, the closer the signal access points are, the denser it is, which evaluates the correctness of the proposal.

In the judgment process, the weighted fusion method in data fusion is adopted for the confidence of the three access points' RSS values, and the weights of the three points are set as follows:

$$\left(\frac{RSSO(O)}{RSSO(O) + RSSA(A) + RSSB(B)}, \frac{RSSA(A)}{RSSO(O) + RSSA(A) + RSSB(B)}, \frac{RSSB(B)}{RSSO(O) + RSSA(A) + RSSB(B)} \right) = (K_1, K_2, K_3) = \left(\frac{34}{94}, \frac{25}{94}, \frac{35}{94} \right) = (0.36, 0.27, 0.37), \quad (21)$$

where the RSS values of the $RSSO(O)$, $RSSA(A)$, and $RSSB(B)$ correspond to the three access points measured at three access points of O , A , and B in order.

In order to prove the effectiveness of the proposed scheme, we use the positioning error indicator to make comparison experiment with the traditional WKNN algorithm and the traditional joint probability algorithm here. The expression of the positioning error is

$$poserr = \sqrt{(x - x_0)^2 + (y - y_0)^2}, \quad (22)$$

where (x, y) represents the estimated coordinates of the

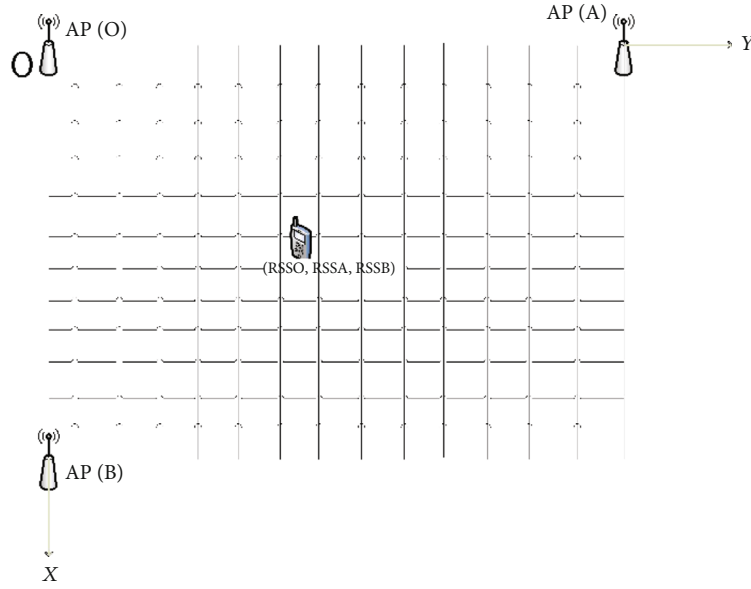


FIGURE 6: The deployment of the access points.

TABLE 2: RSS value of different position.

| (x, y) (m) | (RSSO, RSSA, RSSB) (-dBm) | (X, Y) (m) | (RSSO, RSSA, RSSB) (-dBm) |
|--------------|---------------------------|--------------|---------------------------|
| (0.00, 0.00) | (-34, -74, -82) | (0.86, 0.00) | (-66, -76, -63) |
| (0.00, 0.60) | (-57, -72, -79) | (0.86, 0.60) | (-67, -71, -65) |
| (0.00, 1.20) | (-69, 70, -78) | (0.86, 1.20) | (-74, -70, -66) |
| (0.00, 1.80) | (-78, -62, -75) | (0.86, 1.80) | (-76, -66, -68) |
| (0.00, 2.40) | (-81, -25, -72) | (0.86, 2.40) | (-77, -64, -73) |
| (0.43, 0.00) | (-61, -73, -77) | (1.29, 0.00) | (-70, -75, -35) |
| (0.43, 0.60) | (-63, -68, -76) | (1.29, 0.60) | (-71, -74, -48) |
| (0.43, 1.20) | (-65, -75, -75) | (1.29, 1.20) | (-72, -78, -70) |
| (0.43, 1.80) | (-73, -69, -73) | (1.29, 1.80) | (-75, -77, -66) |
| (0.43, 2.40) | (-71, -58, -70) | (1.29, 2.40) | (-80, -85, -77) |

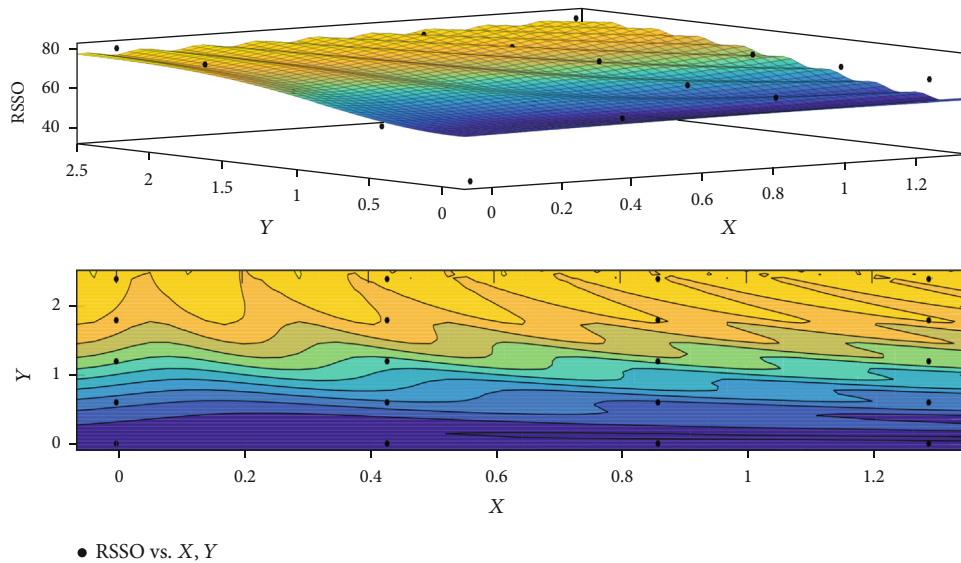


FIGURE 7: Relation between RSSO and position.

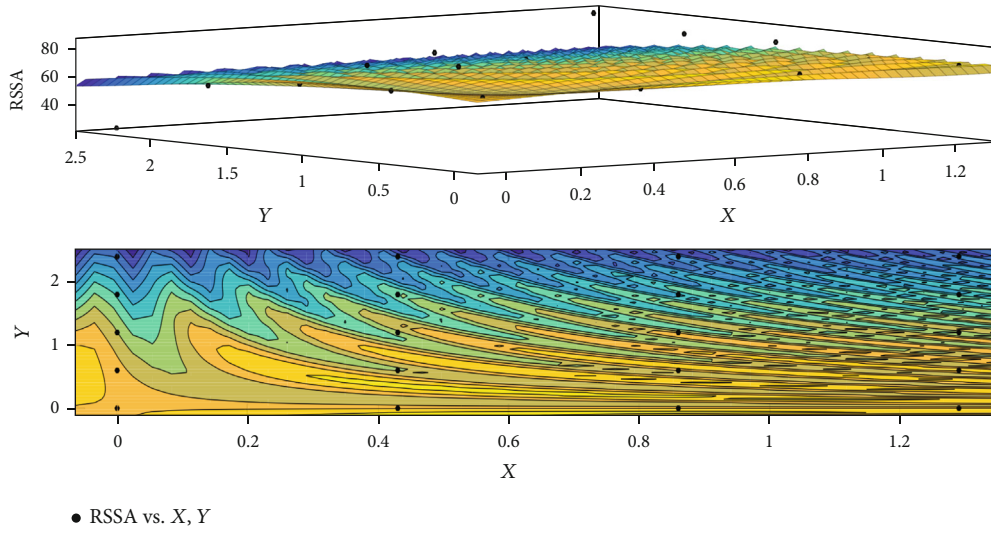


FIGURE 8: Relation between RSSA and position.

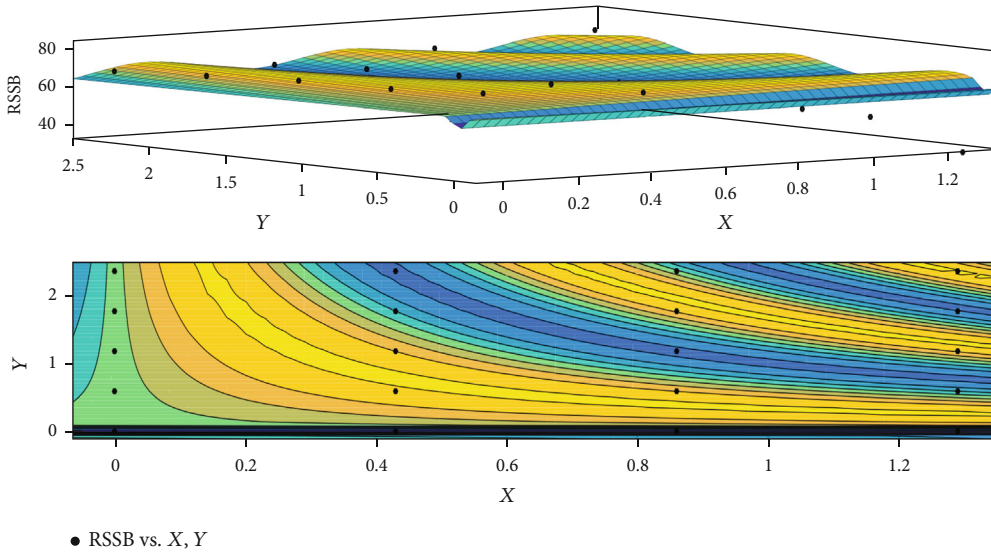


FIGURE 9: Relation between RSSB and position.

object and (x_0, y_0) represents the actual coordinates of the object.

After estimating the position of the object 100 times, the accuracy comparison results of several traditional positioning algorithms are as follows:

- (1) The positioning error of the traditional WKNN algorithm is 0.37 m
- (2) The positioning error of the traditional joint probability algorithm is 0.53 m
- (3) The positioning error of the WKNN algorithm based on the joint probability class is 0.48 m
- (4) The positioning error of our algorithm is 0.25 m

6.3. Indoor Communication Function Verification in Theory. In this subsection, we verify the indoor communication

function in theory. At first, the number of multipath channels is set as 6, the modulation method is BPSK modulation, and the ambient noise is additive white Gaussian noise. The detailed derivation process is listed as following steps.

Step 1. The analog signal after digital-to-analog conversion can be transformed into signal X , which is denoted as follows:

$$X = \begin{pmatrix} a_1 & \cdots & f_1 \\ \vdots & \ddots & \vdots \\ a_6 & \cdots & f_6 \end{pmatrix}. \quad (23)$$

Step 2. After BPSK modulation, the signal can be further expressed as follows:

$$X_M = \begin{pmatrix} a'_1 & \cdots & f'_1 \\ \vdots & \ddots & \vdots \\ a'_6 & \cdots & f'_6 \end{pmatrix}. \quad (24)$$

Step 3. When the data is transmitted through wireless multipath channel, it can be denoted as follows:

$$C = (\text{CSI}_1, \dots, \text{CSI}_6)^T = \begin{pmatrix} a'_1 \cdot m_1 \cdot e^{j\omega t_1} & \cdots & a'_6 \cdot m_6 \cdot e^{j\omega t_1} \\ \vdots & \ddots & \vdots \\ f'_1 \cdot m_1 \cdot e^{j\omega t_1} & \cdots & f'_6 \cdot m_6 \cdot e^{j\omega t_1} \end{pmatrix}, \quad (25)$$

where the model of the wireless multipath channel is

$$(H_1 \cdots H_6) = (m_1 \cdot e^{j\omega t_1} \cdots m_6 \cdot e^{j\omega t_6}), \quad (26)$$

$$h(t) = \sum_{i=1}^6 m_i \delta(t - t_i) \Rightarrow H(\omega) = \sum_{i=1}^6 m_i e^{j\omega t_i}.$$

Step 4. Denote H as the channel matrix

$$H = \begin{pmatrix} H_1 & & 0 \\ & \ddots & \\ 0 & & H_6 \end{pmatrix}. \quad (27)$$

Then, we have

$$C^T = X_M \cdot H, \quad (28)$$

which can also be expressed as follows:

$$H = [X_M]^{-1} \cdot C^T. \quad (29)$$

Based on Equation (27), the multipath transmission function in the wireless channel can be obtained. In addition, under the AWGN conditions, the coefficient matrix K is introduced to improve the accuracy and reliability of the transmission function. Specifically, the effect of introducing the coefficient matrix K mainly focuses on twofold: (1) reduce the effect on the system transfer function after additive Gaussian white noise and (2) reduce the mutual influence between adjacent channels. At this time, denote the coefficient matrix K as follows:

$$K = \begin{pmatrix} k_{11} & \cdots & k_{16} \\ \vdots & \ddots & \vdots \\ k_{61} & \cdots & k_{66} \end{pmatrix}. \quad (30)$$

When taking the additive noise and the influence between adjacent channels into consideration, X_M becomes X'_M , mathematically,

$$X'_M - X_M = \begin{pmatrix} \sigma_{a1} & \cdots & \sigma_{f1} \\ \vdots & \ddots & \vdots \\ \sigma_{a6} & \cdots & \sigma_{f6} \end{pmatrix}. \quad (31)$$

Hence, the following equation holds on:

$$\begin{cases} X_M \cdot H = C^T, \\ X'_M \cdot K \cdot H = C^T. \end{cases} \quad (32)$$

Next, we can use the minimum mean square error criterion to calculate the coefficient matrix K and figure out K to minimize the following equation

$$|C^T T - C^T|^2 = |X'_M \cdot K \cdot H - X_M \cdot H|^2 \Leftrightarrow \left| \begin{pmatrix} k_{11} & \cdots & k_{16} \\ \vdots & \ddots & \vdots \\ k_{61} & \cdots & k_{66} \end{pmatrix} \cdot \begin{pmatrix} a'_1 + \sigma_{a1} & \cdots & f'_1 + \sigma_{f1} \\ \vdots & \ddots & \vdots \\ a'_6 + \sigma_{a6} & \cdots & f'_6 + \sigma_{f6} \end{pmatrix} - \begin{pmatrix} a'_1 & \cdots & f'_1 \\ \vdots & \ddots & \vdots \\ a'_6 & \cdots & f'_6 \end{pmatrix} \right|^2$$

$$= \left| \sum_{i,j=1}^6 K_{ij} \cdot \begin{pmatrix} \sum_{A'=\{a' \dots f\}} A'_i + \sigma_{Ai} \end{pmatrix} - \sum_{A'=\{a' \dots f\}} A'_i \right|^2. \quad (33)$$

At last, the transmission function \hat{H} , which represents the communication function of the wireless communication system, can be determined as follows:

$$\hat{H} = K \cdot H = K \cdot X_M^{-1} \cdot C^T. \quad (34)$$

7. Conclusion and Future Work

The method for realizing indoor positioning and communication based on WiFi signals is of practical significance, and it is not difficult to implement, and the cost is low. This paper proposes a new algorithm for indoor target positioning and communication integration based on WiFi signals. The RSS and CSI values in the WiFi signal are used to achieve indoor target positioning, respectively, and the derived indoor wireless channel system transfer function is used to achieve the purpose of communication. In the positioning part based on the RSS value, the accuracy of the algorithm can reach 0.25 m, which can meet the indoor positioning requirements under certain conditions. In the communication part based on the CSI value, the transmission function of the indoor wireless channel is creatively described using the CSI value. The transmission function of the system is optimized under the conditions of noise and interference between adjacent channels. Finally, the goal of integration of positioning and communication based on WiFi signal level was achieved for the first time. In the next work, we need to further improve this algorithm, taking into account factors such as the movement of people indoors, the

location of access points, and the transmission power of WiFi signals, so that our algorithm is more accurate, and the model we build is more complete to meet the characteristics of indoor complex wireless channel environment.

Data Availability

The RSS data for location used to support the findings of this study are included within the article.

Conflicts of Interest

The authors declare that they have no conflicts of interest.

Acknowledgments

This work is supported by the National Natural Science Foundation of China under Grant 62001126 and in part by the China Postdoctoral Science Foundation (Grant No. 2021M693617).

References

- [1] B. Deebak, F. H. Memon, S. A. Khowaja et al., "Lightweight blockchain based remote mutual authentication for AI-empowered IoT sustainable computing systems," *IEEE Internet of Things Journal*, 2022.
- [2] W. Wang, G. Srivastava, J. C.-W. Lin, Y. Yang, M. Alazab, and T. R. Gadekallu, "Data freshness optimization under CAA in the UAV-aided MECN: a potential game perspective," *IEEE Transactions on Intelligent Transportation Systems*, pp. 1–10, 2022.
- [3] N. Balamurugan, S. Mohan, M. Adimoolam, A. John, T. reddy G, and W. Wang, "DOA tracking for seamless connectivity in beamformed IoT-based drones," *Computer Standards & Interfaces*, vol. 79, article 103564, 2022.
- [4] M. Majid, S. Habib, A. R. Javed et al., "Applications of wireless sensor networks and Internet of Things frameworks in the industry revolution 4.0: a systematic literature review," *Sensors*, vol. 22, no. 6, p. 2087, 2022.
- [5] A. R. Javed, M. U. Sarwar, S. Khan, C. Iwendi, M. Mittal, and N. Kumar, "Analyzing the effectiveness and contribution of each axis of tri-axial accelerometer sensor for accurate activity recognition," *Sensors*, vol. 20, no. 8, p. 2216, 2020.
- [6] Y. Zhang, L. Hsiung-Cheng, J. Zhao, M. Zewen, Z. Ye, and H. Sun, "A multi-DoF ultrasonic receiving device for indoor positioning of AGV system," in *2018 International symposium on computer, consumer and control (IS3C)*, pp. 97–100, Taichung, Taiwan, 2018.
- [7] F. Gonzalez, F. Gosselin, and W. Bachtta, "A 2-D infrared instrumentation for close-range finger position sensing," *IEEE Transactions on Instrumentation and Measurement*, vol. 64, no. 10, pp. 2708–2719, 2015.
- [8] M. U. Ali, S. Hur, and Y. Park, "Wi-Fi-based effortless indoor positioning system using IoT sensors," *Sensors*, vol. 19, no. 7, p. 1496, 2019.
- [9] H. Xu, Y. Ding, P. Li, R. Wang, and Y. Li, "An RFID indoor positioning algorithm based on Bayesian probability and K-nearest neighbor," *Sensors*, vol. 17, no. 8, p. 1806, 2017.
- [10] C. Yang and H.-R. Shao, "WiFi-based indoor positioning," *IEEE Communications Magazine*, vol. 53, no. 3, pp. 150–157, 2015.
- [11] A. Noertjahyana, I. A. Wijayanto, and J. Andjarwirawan, "Development of mobile indoor positioning system application using android and bluetooth low energy with trilateration method," in *2017 International conference on soft computing, intelligent system and information technology (ICSIT)*, pp. 185–189, Denpasar, Indonesia, 2017.
- [12] K. Saleem, M. Saleem, R. Zeeshan et al., "Situation-aware BDI reasoning to detect early symptoms of covid 19 using smart-watch," *IEEE Sensors Journal*, p. 1, 2022.
- [13] Y. Yang, W. Wang, L. Liu, K. Dev, and N. M. F. Qureshi, "AoI optimization in the UAV-aided traffic monitoring network under attack: a Stackelberg game viewpoint," *IEEE Transactions on Intelligent Transportation Systems*, pp. 1–10, 2022.
- [14] Z. Huang, X. Zhu, Y. Lin, L. Xu, and Y. Mao, "A novel WIFI-oriented RSSI signal processing method for tracking low-speed pedestrians," in *2019 5th International Conference on Transportation Information and Safety (ICTIS)*, pp. 1018–1023, Liverpool, UK, 2019.
- [15] S. Tabatabaei, "A novel fault tolerance energy-aware clustering method via social spider optimization (SSO) and fuzzy logic and mobile sink in wireless sensor networks (WSNS)," *Computer Systems Science and Engineering*, vol. 35, no. 6, pp. 477–494, 2020.
- [16] R. Ma, Q. Guo, C. Hu, and J. Xue, "An improved WiFi indoor positioning algorithm by weighted fusion," *Sensors*, vol. 15, no. 9, pp. 21824–21843, 2015.
- [17] B. Wang, X. Liu, B. Yu, R. Jia, and X. Gan, "An improved WiFi positioning method based on fingerprint clustering and signal weighted Euclidean distance," *Sensors*, vol. 19, no. 10, p. 2300, 2019.
- [18] Z.-A. Deng, G. Wang, D. Qin, Z. Na, Y. Cui, and J. Chen, "Continuous indoor positioning fusing WiFi, smartphone sensors and landmarks," *Sensors*, vol. 16, no. 9, p. 1427, 2016.
- [19] C.-H. Hsieh, J.-Y. Chen, and B.-H. Nien, "Deep learning-based indoor localization using received signal strength and channel state information," *IEEE access*, vol. 7, pp. 33256–33267, 2019.
- [20] N. Yu, S. Zhao, X. Ma, Y. Wu, and R. Feng, "Effective fingerprint extraction and positioning method based on crowdsourcing," *IEEE Access*, vol. 7, pp. 162639–162651, 2019.
- [21] S. Lembo, S. Horsmanheimo, M. Somersalo, M. Laukkanen, L. Tuomimaki, and S. Huilla, "Enhancing WiFi RSS fingerprint positioning accuracy: lobe-forming in radiation pattern enabled by an air-gap," in *2019 International Conference on Indoor Positioning and Indoor Navigation (IPIN)*, pp. 1–8, Pisa, Italy, 2019.
- [22] H. Shu, C. Song, T. Pei et al., "Queuing time prediction using WiFi positioning data in an indoor scenario," *Sensors*, vol. 16, no. 11, p. 1958, 2016.
- [23] D. G. Michelson, N. T. Golmie, C. Gentile et al., "A classification scheme for wireless channel models across the development life cycle," in *2019 USNC-URSI Radio Science Meeting (Joint with AP-S Symposium)*, pp. 47–48, Atlanta, GA, USA, 2019.
- [24] A. Kumar, R. Bhattacharjee, and S. Goel, "A clustering based channel model for indoor wireless communication," in *2011 National Conference on Communications (NCC)*, pp. 1–5, Bangalore, India, 2011.

- [25] R. Xu, L. Wang, Z. Geng, H. Deng, L. Peng, and L. Zhang, "A novel wire-wrap slow-wave structure for terahertz backward wave oscillator applications," *IEEE Transactions on Broadcasting*, vol. 64, no. 1, pp. 293–299, 2017.
- [26] A. A. Kalachikov and N. S. Shelkunov, "Construction and validation of analytical wireless MIMO channel models based on channel measurement data," in *2018 XIV International Scientific-Technical Conference on Actual Problems of Electronics Instrument Engineering (APEIE)*, pp. 175–179, Novosibirsk, Russia, 2018.
- [27] R. Stridh, K. Yu, B. Ottersten, and P. Karlsson, "MIMO channel capacity and modeling issues on a measured indoor radio channel at 5.8 GHz," *IEEE Transactions on Wireless Communications*, vol. 4, no. 3, pp. 895–903, 2005.
- [28] X. Liu, C. Liu, W. Liu, and X. Zeng, "Wireless channel modeling and performance analysis based on Markov chain," in *2017 29th Chinese control and decision conference (CCDC)*, pp. 2256–2260, Chongqing, China, 2017.
- [29] S. Lee, Y. Ahn, and H. Y. Kim, "Predicting concrete compressive strength using deep convolutional neural network based on image characteristics," *CMC-Computers Materials & Continua*, vol. 65, no. 1, pp. 1–17, 2020.
- [30] M. Khan and M. K. Jain, "Feature point detection for repacked android apps," *Intelligent Automation and Soft Computing*, vol. 26, no. 4, pp. 1359–1373, 2020.
- [31] B. Deebak, F. H. Memon, K. Dev, S. A. Khowaja, W. Wang, and N. M. F. Qureshi, "TAB-SAPP: a trust-aware blockchain-based seamless authentication for massive IoT-enabled industrial applications," *IEEE Transactions on Industrial Informatics*, p. 1, 2022.